Quantum dot lasers—History and future prospects ⊘

Justin C. Norman ; Richard P. Mirin ; John E. Bowers

Check for updates

CrossMark

View
Online

Export
Citation

Related Content

Mechanisms of Stranski-Krastanov growth

Journal of Applied Physics (February 2012)

Intermixing in Stranski–Krastanov germanium overlayer on Si(100)

Journal of Vacuum Science & Technology A (July 2000)

Stable island arrays by height-constrained Stranski–Krastanov growth

Appl. Phys. Lett. (November 2001)

Quantum dot lasers—History and future prospects

View Online   Export Citation   CrossMark

Justin C. Norman,[1,2] [iD] Richard P. Mirin,[3] [iD] and John E. Bowers[4,a)] [iD]

AFFILIATIONS

[1] Materials Department, University of California, Santa Barbara, Santa Barbara, California 93117
[2] Quintessent Inc., Santa Barbara, California 93117
[3] National Institute of Standards and Technology, 325 Broadway, Boulder, Colorado 80305
[4] Institute for Energy Efficiency, University of California, Santa Barbara, Santa Barbara, California 93117

Note: This paper is part of the Special Topic Collection: Honoring Dr. Art Gossard's 85th Birthday and his Leadership in the Science and Technology of Molecular Beam Epitaxy.
[a)]Electronic mail: bowers@ece.ucsb.edu

ABSTRACT

We describe the initial efforts to use molecular beam epitaxy to grow InAs quantum dots on GaAs via the Stranski–Krastanov transition and then discuss the initial efforts to use these quantum dots to demonstrate quantum dot lasers. We discuss the developments in quantum dot lasers over the past 20 years and the future prospects for these lasers for scientific and commercial applications.

I. INTRODUCTION

Soon after the demonstration and development of quantum well (QW) lasers (one dimension of quantum confinement), researchers began to consider how additional quantum confinement such as two degrees (quantum wire) and three degrees [quantum dot (QD)] would affect the semiconductor laser properties. In 1982, Arakawa and Sakaki[1] proposed that "multidimensional quantum well" lasers would have greatly increased characteristic temperatures. Shortly thereafter, a high material gain and low threshold current density were predicted by Asada *et al.*[2] for hypothetical "quantum boxes" in III–V material systems. These initial theoretical predictions of improved laser performance in what would later be referred to as quantum dots come from the modifications of the density of states. This is straightforward to understand if you assume that the QDs are ideal-all identical, with large ($>2\,k_bT$) intraband spacing between states. The large characteristic temperature is a consequence of the Fermi distribution of the carriers—nearly all injected carriers will be in the ground state of the QDs and will provide gain at the lasing wavelength. Also, every additional electron injected once threshold is reached goes into the lasing mode, resulting in extremely large differential gain.

These enticing performance gains that were theoretically predicted in the 1980s were a significant reason for the search for techniques that could fabricate high density, high uniformity QDs from III–V semiconductors, but as experimentally viable material

systems were developed for achieving zero-dimensional confinement, harsh realities became apparent through the inhomogeneities inherent to epitaxial dot layers and the reduced confinement of holes relative to electrons in technologically relevant materials.

Quantum dot research at the University of California at Santa Barbara (UCSB) started in the molecular beam epitaxy (MBE) lab overseen by Prof. Art Gossard, with significant collaboration from many other UCSB professors (Kroemer, Petroff, Coldren, Bowers, Speck). Dr. Mohan Krishnamurthy, a postdoctoral researcher for Prof. Petroff, had previously done research on the growth of Ge on Si[3] and shown that this highly strained system grew in the Stranski–Krastanov (layer + island) growth mode. Krishnamurthy proposed that InAs on GaAs might grow in a similar fashion, where no dislocations form if the growth is terminated shortly after island formation.[4] This led to the first demonstration of InAs QDs at UCSB, research which was presented at the North American Conference on Molecular Beam Epitaxy at Stanford in September 1993.[5] These results were published later that year,[6] followed shortly afterward by similar results by Moison *et al.*[7] Although these two results started the revolution in self-assembled QD growth of III–V semiconductors that continues until this day, we note there was evidence (photoluminescence and transmission electron microscopy) as early as 1985[8] that MBE growth of thin InAs layers led to the formation of QDs, and there was strongly suggestive evidence of island formation during the initial growth of InAs

on GaAs from RHEED in 1982.[9] It was in this same timeframe of the mid-1990s that the atomlike density of states was first verified in single QDs via photo- and cathodo-luminescence techniques.[10,11]

Although the prospects of high characteristic temperature, lower threshold currents, and large differential gain were extremely desirable for high performance lasers, another desirable property emerged soon after the first demonstration of QDs by MBE, namely, the ability to increase the size of the QDs to enable room temperature emission at 1300 nm on GaAs.[12] We used a variant of conventional III–V MBE in which the Group III elements were deposited without arsenic, which led to strong surface segregation of the indium and eventual formation of QDs. By simply continuing the growth until the islands reached a sufficient size, we were able to demonstrate this desirable long wavelength emission. This was viewed at the time as an important step toward making 1300 nm in-plane lasers for fiber optics as well as vertical-cavity surface-emitting lasers (VCSELs) with a single epitaxial growth, similar to what had been demonstrated with 980 nm VCSELs.

Room temperature lasing from QDs was achieved in 1996.[13–16] The work at UCSB on broad area, pulsed operation from 80 to 295 K clearly demonstrated strong state-filling at higher temperatures and shorter laser lengths. We demonstrated that the lasing wavelength could be almost independent of the temperature [Fig. 1(a)]. This result was a consequence of the state-filling compensating for the change in the bandgap. Similarly, the lasing wavelength was independent of mirror loss [Fig. 1(b)]. Both results showed unique properties of quantum dots compared to quantum wells for lasers. These lasers operated between 1000 and 1100 nm, important for seeding fiber amplifiers at 1060 nm and paving the way for the demonstration of room temperature lasing at 1310 nm a couple of years later.[17]

The uniformity of the ensemble of QDs was never good enough to achieve the vision of nearly infinite characteristic temperatures for operating regimes well above room temperature, and

the high differential gain that was first envisioned for QD lasers never manifested, leaving QW devices the superior candidate for direct modulation. Nevertheless, many interesting laser properties were demonstrated in the first several years and performance rapidly grew to rival QW lasers. Figure 2 shows state-of-the-art threshold current density for semiconductor lasers by publication year starting from the earliest demonstrations of double-heterostructure (DH)[18,19] lasers and scaling to higher dimensions of quantum confinement in QWs[20–25] and with QDs ultimately winning out due to their ultralow transparency current densities.[14,26–28]

One important property that was largely neglected in the early literature was the reduced ambipolar diffusion of injected carriers[29] in QD layers. This property would soon become useful for the demonstration of QD lasers grown directly on silicon and in small footprint microring and disk cavities with a high surface area to volume ratio.[30] The effects of defect tolerance are shown in Fig. 2 where quantum dot lasers grown on Si (see Ref. 31 for a brief history of the referenced QW and QD lasers on Si) are able to rival native substrate devices and could open the door to the long-sought epitaxial cointegration of III–V light sources with silicon.

Today, the most well-studied quantum dot material system is that of InAs/GaAs, often embedded in an InGaAs quantum well in order to extend the emission wavelength to the technologically important O-band for optical communications. Figure 3 gives a schematic band structure for this material system as well as a representative atomic force microscope and a cross-sectional scanning transmission electron microscope (TEM) image of these dots. While these images could represent typical high performance lasers from the literature, the kinetic nature of QD growth allows for extensive tunability of the dot size, shape, and density allowing for the band structure and density of states to be effectively tuned for a particular application.

In this review, we emphasize the outcomes of the early experimental demonstrations and theoretical hypotheses described above
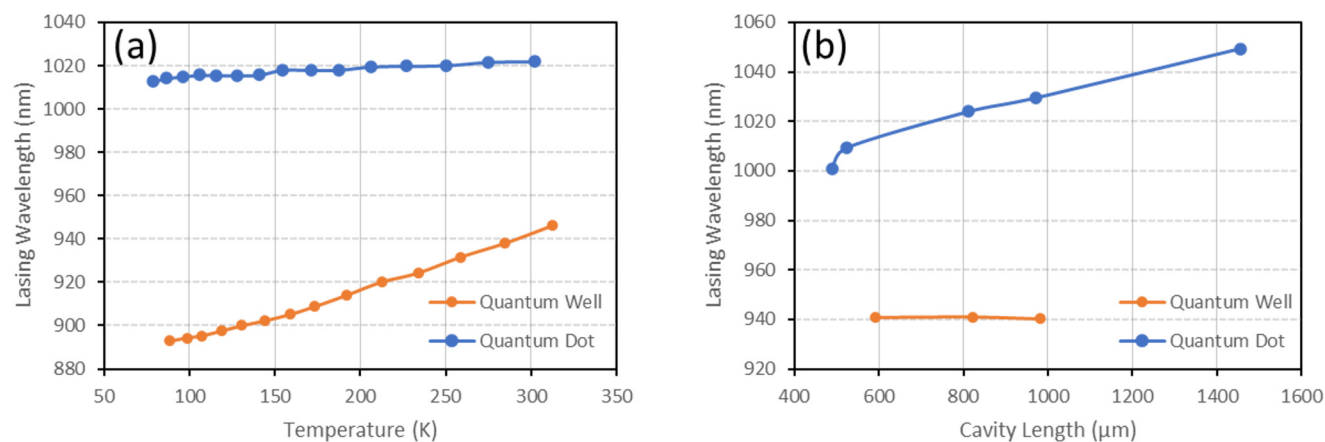
FIG. 1. Lasing wavelength is plotted as a function of (a) temperature and (b) cavity length for quantum dot and quantum well lasers. The nearly constant wavelength vs temperature and varying wavelength vs cavity length are consequences of state-filling in quantum dot lasers. Adapted with permission from Mirin *et al.*, Electron. Lett. **32**, 1732 (1996). Copyright 1996, Institution of Engineering and Technology.
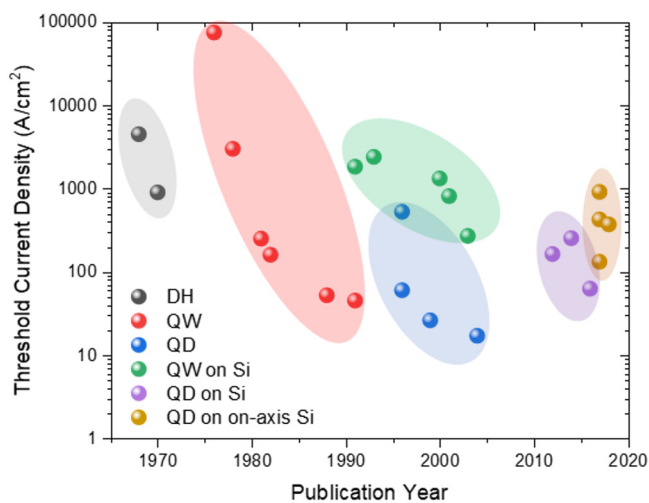
FIG. 2. Threshold current density vs publication year is plotted for semiconductor lasers starting with DH and then moving to increasing dimensions of quantum confinement. Results for QW and QD lasers are shown for growth on native substrates and Si with the most recent results moving to CMOS-standard on-axis Si as opposed to the miscut substrates used previously.

in generating devices of significant and current technological interest that outperform anything that can be achieved in similar quantum well devices. The topics covered below represent the most significant areas of QD laser research today. That said, the field could not have transitioned from its not-so-humble beginnings of infinite promise to its current status of still remarkable achievement without the extensive efforts of many groups around the globe working on fundamental research in material growth, low-dimensional physics and materials science, and optical communications. For detailed reviews of QD lasers (and other devices) at

various times in the history of the field, we refer the interested reader to Refs. 31–42.

II. ADVANTAGES OF QUANTUM DOT LASERS

There are five primary reasons to use quantum dots rather than quantum wells for the gain region of a laser. These will be discussed in more detail later. The advantages are

(1) higher temperature operation,
(2) lower linewidth enhancement factor and reduced linewidth,
(3) reduced reflection sensitivity,
(4) improved mode-locking, and
(5) reduced sensitivity to defects.

These advantages have been demonstrated, primarily in the InAs/GaAs material system. Early papers on quantum dot lasers suggested other advantages, such as higher modulation speeds. The modulation capability of quantum dot lasers has yet to exceed that of quantum wells in any demonstrated material system, primarily because of the reduced confinement factor and increased damping in quantum dot gain regions. That said, many modern photonic technologies have migrated to integrated platforms where external modulation can provide superior speeds and energy efficiency to direct modulation, such that the pros and cons of QDs compared to QWs become even more one-sided.

The theoretical advantages of QD lasers over QW lasers took several years to be realized following their initial development, with the primary barrier being inhomogeneous broadening. As growth techniques improved and various groups undertook the extensive optimization efforts required to achieve high performance, many breakthroughs in laser (and amplifier) performance materialized. The highest impact developments include record high temperature operation for a semiconductor laser, ultralow linewidth enhancement factors for insensitivity to optical feedback and narrow linewidths, high performance mode-locking with subpicosecond pulsewidths and low jitter, and an insensitivity to crystalline defects
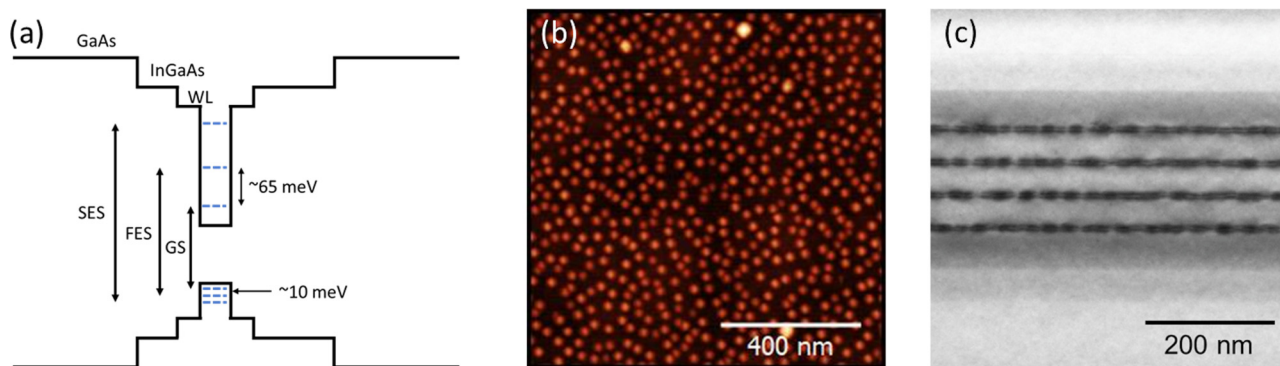
FIG. 3. (a) Schematic band structure representative of an InAs quantum dot in an InGaAs quantum well surrounded by GaAs, which is representative of the most well-studied quantum dot implementation to date. These dots show three confined levels labeled as the ground state (GS), the first excited state (FES), and the second excited state (SES). Due to their Stranski–Krastanov growth mode and intermixing during growth, there is an additional quantum well that is typically referred to as the wetting layer (WL). (b) An atomic force micrograph of uncapped InAs quantum dots is shown. (c) A cross-sectional scanning transmission electron micrograph is shown displaying five layers of InAs quantum dots making up a laser's active region.

that allows for heteroepitaxy on Si or other metamorphic buffers while maintaining performance and reliability. These areas are all the subject of ongoing and rapidly accelerating research and will likely show substantial advancement in the years to come, most notably through photonic integration, which has enabled significant improvements in performance and functionality for quantum well based devices over the last 15 years.

III. HIGH TEMPERATURE LASERS

Quantum dot lasers were originally predicted to possess invariant threshold currents with increasing temperatures (high characteristic temperatures). This comes about from the inability of carrier populations to thermally redistribute across the delta-functionlike density of states. Two primary challenges prevent real materials from matching this idealization. The first challenge comes in suppressing the inhomogeneous broadening to a level that minimizes overlap between neighboring levels, which would create a quasicontinuum in the density of states. The second challenge relates to the first and is that the conduction and valence band offsets are highly asymmetric in the most epitaxially mature material systems, InAs/GaAs and InAs/InP, with the hole states being far less confined than the electron states.[43] The latter issue has been well remedied through p-type modulation doping in the quantum dot active region to offset the effects of thermalization.[44,45] Nevertheless, state-of-the-art performance remains tied to extremely narrow regions of the growth parameter space necessitating extensive growth optimization campaigns and precise control of growth conditions.

In the InAs/GaAs system, a photoluminescence full-width-at-half-maximum of ~24 meV at room temperature and a ground-to-first-excited-state energy separation of 80 meV led to demonstration of 220 °C continuous wave lasing [Fig. 4(a)],[46] the highest of any semiconductor laser to date. The threshold was also very stable, increasing from 15 mA to only 27 mA as the temperature increased from 30 to 125 °C (characteristic temperature, $T_0 = 170$ K). This temperature range covers the technologically relevant operating conditions in datacenters and supercomputers where high temperature stability simplifies laser control and low thresholds improve efficiency. Similar lasers were used in the demonstration of an athermal silicon optical interposer operating up to 125 °C with error-free channels operating at 20 Gbps.[48] Similar performance has also been obtained at a shorter wavelength of 850 nm, where vertical-cavity surface-emitting lasers with maximum operating temperatures >200 °C have been demonstrated with maximum direct modulation data rates of 25 Gbps at 180 °C.[49] This same material system has been used for lasers grown on Si demonstrating 110 °C continuous wave operation from the dot ground state and 119 °C lasing from the excited state [Fig. 4(c)].[50]

Similar results have been obtained using C-band InAs/InP quantum dots. Abdollahinia et al.[47] have reported continuous wave lasing up to 120 °C and pulsed lasing to 195 °C. Curves up to 80 °C are reproduced in Fig. 4(b). This laser exhibits threshold characteristic temperatures of 100–144 K from 20–100 °C and was directly modulated at a data rate of 26 Gbps at 80 °C. This performance was also enabled through extensive efforts to reduce inhomogeneous broadening and increase dot density,[51] which is more challenging in the InAs/InP system due to the tendency of the InAs to form elongated, highly nonuniform dashlike structures.

IV. LOWER LINEWIDTH ENHANCEMENT FACTOR

The linewidth enhancement factor is one of the most important figures of merit in semiconductor laser performance.[52] The parameter, usually represented as α or α_H, is defined as the ratio of the differential refractive index change with carrier density, dn/dN,
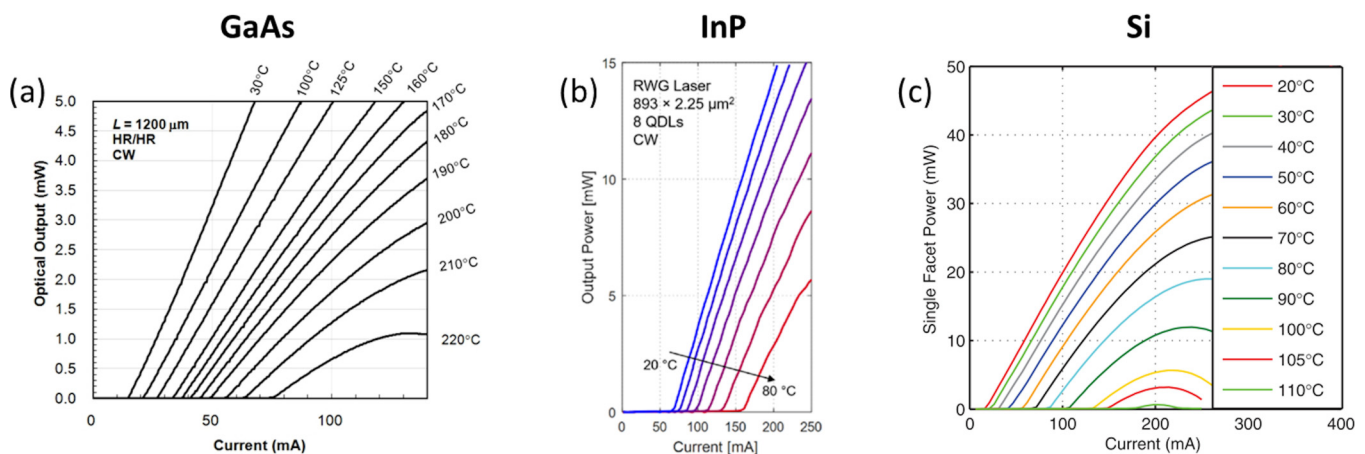

FIG. 4. Record-setting high temperature continuous wave power output vs bias current curves are shown for quantum dot lasers grown on (a) a GaAs substrate that reaches 220 °C (Ref. 46) (Kageyama et al., *The European Conference on Lasers and Electro-Optics (CLEO)*. Copyright © 2011 by Optical Society of America. Reprinted by permission of Optical Society of America), (b) an InP substrate reaching up to 120 °C (Ref. 47) (reprinted with permission from Abdollahinia et al., Opt. Express **26**, 6056 (2018). Copyright 2018, The Optical Society), and (c) a silicon substrate reaching 110 °C from the ground state and 119 °C from the excited state. Reprinted with permission from Liu et al., Appl. Phys. Lett. **104**, 041104 (2014). Copyright 2014, American Institute of Physics.

to the differential gain, dg/dN,

$$\alpha = -\frac{4\pi}{\lambda}\left(\frac{dn}{dN}\right)\left(\frac{dg}{dN}\right)^{-1}.$$

Semiconductor laser linewidths ($\Delta\nu \propto \alpha^2$) and a laser's susceptibility to optical feedback (coherence collapse threshold $f_{crit} \propto \alpha^{-4}$) are both tied to this parameter.[53] A laser's linewidth and stability (i.e., noise) determine the error-free data rates that can be achieved in optical communications, and in optical sensing, they dictate detection sensitivity. In integrated photonic systems, parasitic reflections are unavoidable, necessitating the inclusion of an optical isolator to stabilize laser performance. Optical isolators are expensive, bulky, and lossy, which makes them undesirable, and the reduced feedback sensitivity of QD lasers renders the isolator unnecessary in most applications.

The Kramers–Kronig relations suggest that the symmetric density of states of quantum dots should yield vanishing α factors, and early calculations for idealized structures further supported this hypothesis.[54] However, in real QD systems, interactions between QD states and those of the surrounding matrix and inhomogeneous broadening increase α.[55] Nevertheless, it only took a few years after the first laser demonstrations for ultralow linewidth enhancement factors of 0.1 to be observed,[56] and recent calculations suggest that there could be regimes of operation with vanishing α at the laser gain peak.[57] Typical values of α in QW lasers are from 3 to 5 near threshold. A relative comparison (subthreshold) of QD lasers on GaAs/Si with a commercial off-the-shelf QW laser is given in Fig. 5. Figure 5(b) shows the spectral dependence of α in a C-band QD laser on InP; it is notably higher than that of GaAs

due primarily to the increased inhomogeneous broadening typically observed in QDs on InP.[58]

Recent experimental works have confirmed the benefits of QD-based active regions and their low α. Narrow linewidth distributed feedback (DFB) lasers have been demonstrated in C-band InAs/InP with linewidths of 60 kHz[59] and in O-band InAs/GaAs Fabry–Perot lasers grown on Si with Lorentzian linewidths of 480 kHz.[60] These results are well below typical values in standalone QW DFBs where linewidths can easily reach the megahertz regime.

V. REDUCED REFLECTION SENSITIVITY

As mentioned above, parasitic reflections can have major detrimental effects on laser noise, an effect that is mediated by the linewidth enhancement factor and the degree of damping in the laser oscillation. Quantum dots exhibit both ultralow α and overdamped relaxation oscillations making them highly resilient against reflections.

The highly damped relaxation oscillations observed in quantum dot lasers result from inhomogeneous broadening and their relatively closely spaced hole energy levels,[61] an effect mitigated by modulation p-doping. While this characteristic has been a disadvantage toward achieving high speed direct modulation—at least with regard to outperforming state-of-the-art quantum wells—it has enabled low relative intensity noise (RIN) in quantum dot devices. In both C-band and O-band devices, RIN levels as low as −160 dB/Hz have been achieved.[62,63] Even in quantum dot lasers grown on Si, where Shockley–Read–Hall recombination should increase noise, minimum RIN levels of −150 dB/Hz have been obtained.[64]

A semiconductor laser's sensitivity to reflections is most often quantified in terms of its critical feedback level for coherence collapse, f_{crit}, according to the derivation of Helms and Petermann.[65] In the low α regime, this gives a functional dependence of
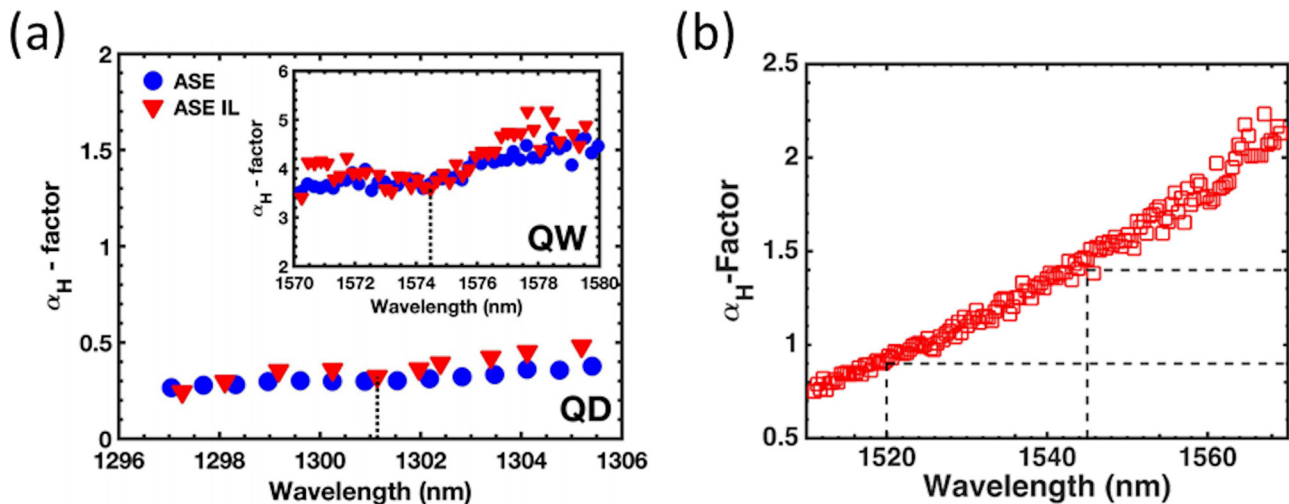

FIG. 5. Linewidth enhancement factor is plotted for (a) a p-type modulation doped quantum dot laser on GaAs/Si, for a commercial off-the-shelf quantum well laser (inset), and (b) for a quantum dot laser on InP. The measurements were obtained subthreshold from amplified spontaneous emission (ASE) spectra and a complementary injection-locking (IL) technique [in (a)] to further support the result. Figure 5(a) is reprinted with permission from Duan *et al.*, Photonics Res. **7**, 1222 (2019). Copyright 2019, The Optical Society. Figure 5(b) is reprinted with permission from Duan *et al.*, Appl. Phys. Lett. **112**, 121102 (2018). Copyright 2018, American Institute of Physics.
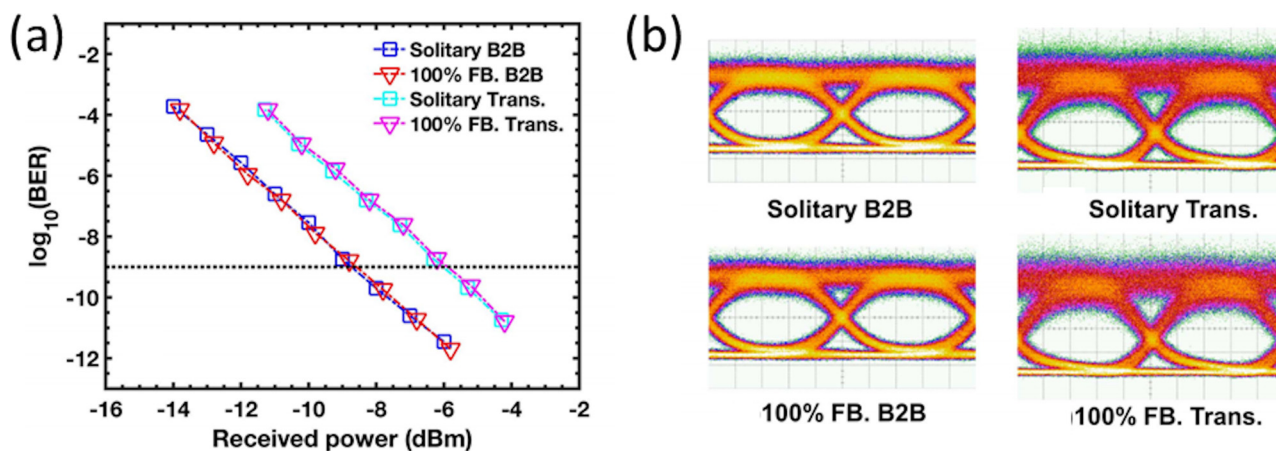
FIG. 6. (a) Bit error ratio (BER) curves are plotted for a quantum dot laser transmitting at 10 Gb/s via external modulation with and without optical feedback (FB) generated by an external 100% back-reflector (re-entrant power of −7 dB in the laser cavity). In both B2B and 2 km transmission configurations, there is no power penalty associated with feedback. (b) Eye diagrams are shown for the solitary laser without feedback and with 100% back-reflection in B2B and 2 km transmission configurations. Reprinted with permission from Duan *et al.*, Photonics Res. **7**, 1222 (2019). Copyright 2019, The Optical Society.

$f_{crit} \propto \gamma^2 \alpha^{-4}$, clearly demonstrating an extreme sensitivity to α and significant dependence on the damping factor, γ. In O-band quantum dot lasers grown on Si, the absence of coherence collapse has been observed at back-reflection levels of 100% thanks to their ultralow linewidth enhancement factors.[66–68] This unprecedented level of stability provides a pathway to isolator-free high performance and low cost photonic integrated circuits.[69] The results of a transmission experiment with an externally modulated QD laser at 10 Gb/s is shown in Fig. 6 for back-to-back (B2B) and 2 km transmission distances. In both cases, there is no observed power penalty associated with the insertion of a 100% back-reflector in front of the laser (after a 10% tap for measurement),[70] and clearly open eyes are observed in all cases.

VI. HIGH PERFORMANCE MODE-LOCKING

Mode-locked lasers represent a special class of lasers where a fixed phase relationship exists between the lasing modes propagating in the cavity. This fixed phase relationship leads to optical pulses in the time domain and a comb of equally spaced lasing modes in the frequency domain, with the frequency spacing set by the round-trip time of the optical cavity. The fact that the modes are all equally spaced with a spacing set by an easily controlled design parameter makes mode-locked lasers ideal candidates for wavelength division multiplexed systems. Additionally, the pulsed time-domain emission is potentially useful for multiphoton microscopy and tomography.

In general, a laser can be forced into a mode-locked regime by using a saturable absorber at one end of the cavity (termed fundamental mode-locking) or at some integer divisor of the cavity length (termed harmonic mode-locking or colliding pulse mode-locking). The absorber can be modulated (active mode-locking) or held at constant bias (passive mode-locking). In colliding pulse

mode-locking, the frequency spacing (pulse rate) is set by the placement of the absorber. For example, absorbers placed at ¼ of the cavity length would multiply the frequency spacing by four, and there would be four pulses simultaneously propagating in the cavity. The additional Fabry–Perot modes between the mode-locked lines are suppressed in this case. A third class of a semiconductor mode-locked laser that has been demonstrated almost exclusively in quantum dot devices entirely omits saturable absorbers and shows spontaneous locking of the lasing modes over some range of bias current. This last case is not very well understood but may result from enhanced four-wave mixing in quantum dot active regions,[71] but it is highly desirable as a candidate for highly efficient mode-locked lasers since it would not incur losses from a saturable absorber. Quantum dots have proven themselves extremely useful for mode-locked laser applications due to their inhomogeneous broadening and fast gain/absorption recovery.[72] In contrast to the other applications discussed in this review, mode-locked lasers benefit from a dispersion of quantum dot emission energies acting independently of each other. In many cases, the ideal case for mode-locked laser performance would be to generate a broad spectrum, flat-top frequency comb. Here, the inhomogeneous broadening provides the obvious benefit of a broader emission spectrum, but it could provide additional benefits by reducing mode-partition noise. Multiwavelength lasers experience intensity noise on each of the lasing modes as power shifts between modes within the homogeneous broadening of the gain material. With sufficient inhomogeneous broadening, distant portions of the lasing spectrum will begin to decouple from each other, limiting this effect. The ultrafast gain/absorption recovery in quantum dots allows for ultrashort pulse generation (subpicosecond) and high repetition rates.

Successful demonstrations of quantum dot mode-locked lasers have been shown in both InAs/GaAs (including on Si substrates)
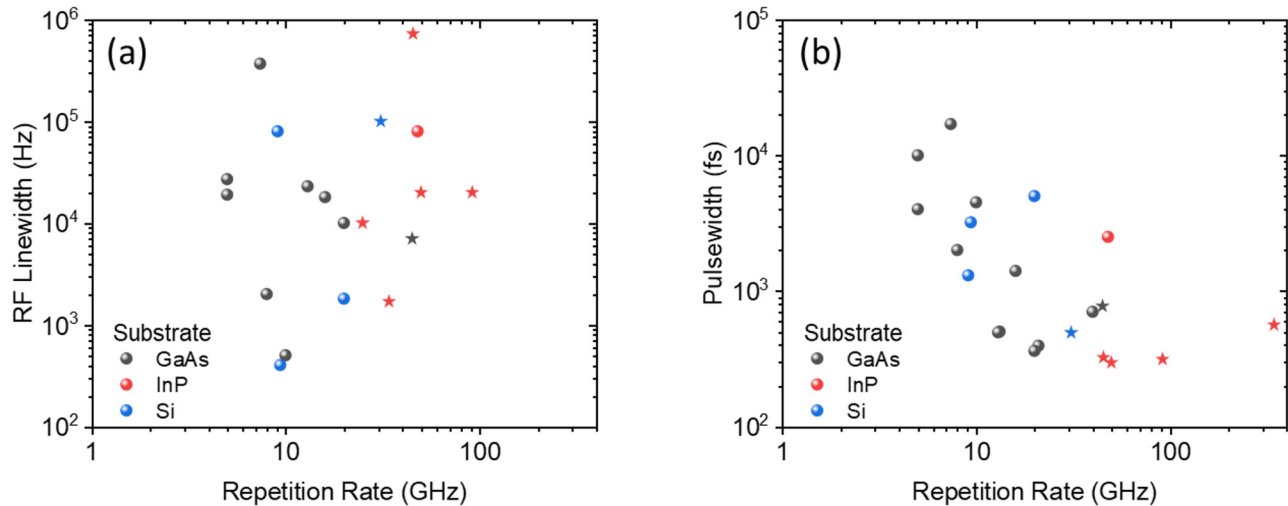
FIG. 7. Survey of mode-locked laser figures of merit for quantum dot lasers grown on GaAs, InP, and Si substrates is shown including (a) the radiofrequency (RF) linewidth of the beatnote as a function of the cavity repetition rate and (b) the time-domain pulsewidth as a function of the cavity repetition rate. Datapoints indicated by stars represent single-section mode-locked lasers (no saturable absorber). The sampled references include Refs. 73–76, 79, and 81–97.

and InAs/InP material systems with the latter holding most of the performance records. Both systems have shown single-section mode-locking resulting in subpicosecond pulsewidths.[73–77] Most notably, the shortest pulsewidth ever obtained in a semiconductor mode-locked laser was obtained in such a device at 295 fs, obtained with an external differential efficiency of 30%.[73] The broad frequency combs make these light sources ideal for single-emitter Tbps transmission systems,[78–80] which should dramatically improve cost and reliability over incumbent technology, which is based around arrays of single wavelength lasers. Quantum dot lasers also hold the record for lowest integrated timing jitter with 82.7 fs in the ITU telecommunication standard band from 4 to 80 MHz.[78] Low timing jitter is beneficial in applications such as clock distribution and recovery, analog-to-digital conversion, and radiofrequency (RF) signal generation. A summary of mode-locking figures of merit across the QD material systems and substrates is given in Fig. 7.

VII. DEFECT TOLERANT LASERS

Quantum dot lasers exhibit a unique insensitivity to crystalline defects, such as dislocations and point defects, that makes them uniquely suited to heteroepitaxial integration and operation in harsh environments. The origin of quantum dots' defect tolerance results from a combination of the in-plane quantum confinement and reduced diffusion lengths of charge carriers outside the dots as well as a potential mechanical hardening of the crystal lattice in the vicinity of the dots. These characteristics are likely the missing piece to finally achieving the holy grail of economical manufacturability that is epitaxial integration of III–V light sources on silicon, and they could enable new long-lifetime devices to operate in high radiation environments such as space or particle accelerators.[98]

Traditionally, semiconductor laser failure is often the result of so-called dark-line defects (DLDs), which describe regions of high nonradiative recombination that start at a point (e.g., processing defect, grown-in dislocation, etc.) and grow during device operation to consume the laser active region.[99] The microscopic structure of a DLD is a dendritic network of dislocations that has grown through recombination enhanced dislocation climb (REDC) and glide (REDG) processes. The barrier to dislocation climb and glide is too high to overcome at reasonable operating temperatures; therefore, it requires recombination of electron-hole pairs to provide the necessary energy. By preventing carrier diffusion to existing dislocations (or point defect clusters that could nucleate dislocation loops), laser lifetime can be extended as REDC and REDG are suppressed.

The three-dimensional quantum confinement of quantum dots helps to trap carriers that could have otherwise migrated to a dislocation to recombine. Furthermore, these inhomogeneities in the surrounding material dramatically reduces in-plane carrier diffusion lengths for unconfined carriers to ~500 nm.[100] Together, these two effects, along with inherently low threshold currents, make quantum dots particularly resilient to nonradiative recombination. Specifically examining the case of heteroepitaxial growth of InAs/GaAs quantum dot lasers on silicon, the performance difference between quantum dot and quantum well devices is stark. Direct comparisons have been made both experimentally[101,102] and theoretically,[103] suggesting that quantum well lasers cannot achieve acceptable performance levels until reaching near native substrate levels of dislocation density. Even then, the rapid REDC that can occur in QW devices means that a single dislocation in a device can cause failure.[104] This is further supported by the relatively low device efficiencies and poor lifetimes achieved in quantum well devices despite heroic epitaxial growth efforts in the 1980s and 1990s.[31,105] In contrast, recent advancements in quantum dot lasers
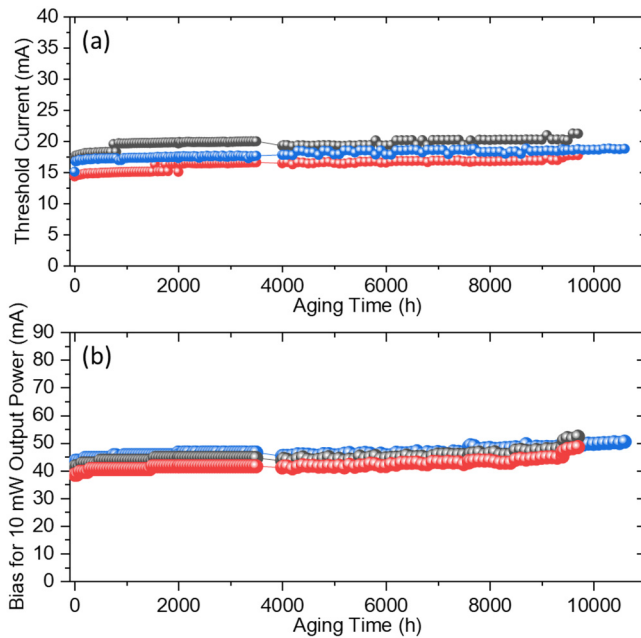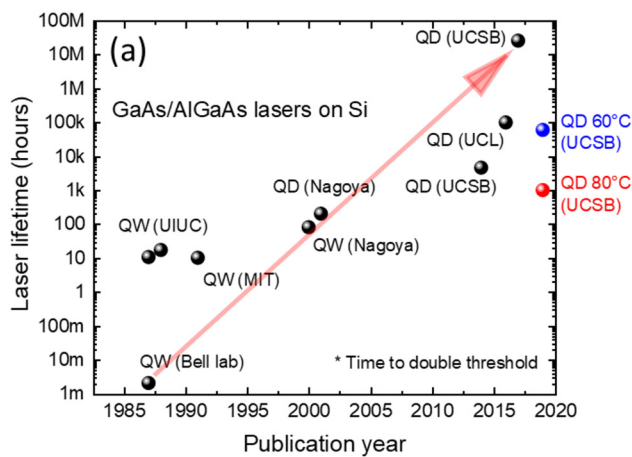
FIG. 8. Degradation in (a) threshold current and (b) operating current for 10 mW output power is plotted over time for three lasers grown on silicon with a dislocation density of ∼7 × 10⁶ cm⁻². The lasers were aged continuously at twice their initial threshold current and 35 °C for 10 000 h. These data represent a continuation of the results in Ref. 106.

even at 60 °C.[108] This performance represents a nearly four order of magnitude improvement in just the last five years, and recent discoveries and improved understanding of the failure mechanisms in these devices suggest that similarly rapid improvements will be maintained in the years to come. A summary of laser lifetimes for devices grown on Si is shown in Fig. 9(a) where the recent rapid progress enabled by quantum dots is apparent. In Fig. 9(b), QD laser reliability is plotted for various temperatures and dislocation densities alongside a datapoint for a native substrate material. This plot emphasizes that while current results are very promising to future commercial viability, more work remains to be done as the gap between native substrate lasers and those grown on silicon is still multiple orders of magnitude in performance, and commercial applications need reliability at high temperatures to avoid impractical cooling requirements for on-chip light sources.

Recent notable findings include fundamental advancements in the material science of quantum dot laser degradation as well as empirical device observations for how to improve performance. Detailed studies using cathodoluminescence and TEM imaging of aged and unaged quantum dot lasers reveal that dislocation climb does occur, but that it is highly suppressed, and suggests that the primary degradation mechanism is a uniform decrease in radiative efficiency throughout the material, including away from dislocations.[109] By analyzing the structure of dislocation climb segments, Mukherjee et al. found strong evidence that the degradation is not primarily due to the extension of the dislocation lines themselves but rather from the emission of vacancy clouds expelled during dislocation climb that diffuse through the material. This is consistent with the observed $t^{0.5}$ degradation rate in quantum dot layers, which is suggestive of a diffusion based process.[110,111] Another observation previously neglected in the literature is that threading dislocations in quantum dot lasers on silicon leave behind long (potentially 10 s of microns) misfit segments in the laser active region.[109,112,113] These misfits have a much larger interaction cross

have shown extreme promise with virtually degradation free operation observed near room temperature (Fig. 8) at dislocation densities as high as 7 × 10⁶ cm⁻² (Refs. 106 and 107) and promising extrapolated device lifetimes of several 10 s of thousands of hours
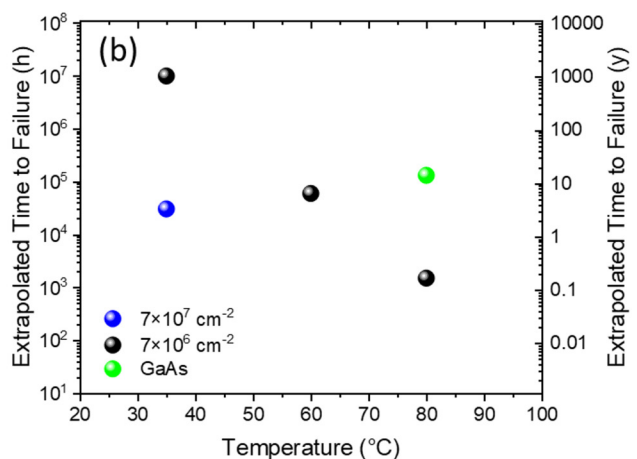

FIG. 9. (a) Historical results for measured or extrapolated device lifetimes for lasers grown on silicon. The black datapoints all represent aging near room temperature. (b) Extrapolated time to failure for quantum dot lasers grown on silicon at two dislocation densities compared with a nominally identical laser grown on GaAs at various aging temperatures. Figures adapted from Jung et al., Phys. Status Solidi A **216**, 1800602 (2018). Copyright 2018, John Wiley & Sons, Inc.; Norman et al., IEEE J. Quantum Electron. **55**, 2001111 (2019). Copyright 2019, John Wiley & Sons, Inc.; and Norman et al., Proc. SPIE **11285**, 1128504 (2020). Copyright 2020, SPIE.

section with the dot layers than do threading segments, which have been the focus of previous work. Selvidge *et al.* have recently identified these misfits as originating from thermal expansion coefficient mismatch during growth cooldown and have developed a novel technique of removing the misfits from the laser's intrinsic region through insertion of dislocation trapping layers in the doped cladding.[114] In their materials, the misfit segments form in the majority carrier regions of the doped cladding and should be relatively innocuous due to the limited minority carrier populations available for nonradiative recombination. Using their techniques, they were able to show near native substrate level initial performance at a high dislocation density of 3×10^7 cm^{-2}. Reliability data are not yet reported, but a 95% reduction in misfit length in the laser active region was observed, which would yield orders of magnitude improvements in reliability based on extrapolation from studies of quantum dot reliability as a function of dislocation density.[106] An additional empirical observation has been made that the mean-time-to-failure (MTTF), which is commonly expressed by the relationship $MTTF \propto J^{-n}\exp(E_A/kT)$ with J as the current density, kT as the thermal energy, and n and E_A as the experimental fitting parameter and activation energy, respectively, possesses a current density exponent $n = 4$ and activation energy $E_A = 0.9$ eV.[111] In fact, the current world records for reliability at elevated temperatures[115,116] were obtained at 2–4× threshold, which gave output powers of ∼20 mW. Many applications could require lower output power and, thus, lower bias currents. This current exponent suggests that more reliable lasers on Si should emphasize longer, low loss cavity designs.

Beyond tolerance to dislocations, quantum dots also show improved resilience to defects generated by high energy ionizing radiation.[117,118] The enhanced radiation hardness of dots relative to wells can likely be attributed to the same effects that enhance laser reliability in the presence of dislocations. Direct comparisons of dot and well luminescence before and after exposure to radiation revealed 2–3 orders of magnitude less degradation in the quantum dot sample. This is very promising for space-based applications, military applications, and for use in other high radiation environments such as particle accelerators such as CERN where their detectors would benefit from the high data rates achievable using photonic systems.[98]

VIII. SUMMARY AND FUTURE PROSPECTS

Quantum dot lasers have come a long way since their initial conception in 1982. The first devices were formed in the InAs/GaAs material system and improved rapidly through careful optimization and improvement in growth techniques. The majority of the growth development to date emphasized narrow inhomogeneous broadenings, which enabled experimental realizations of low threshold, high temperature operation and low noise, feedback insensitive operation. Over time, QD development expanded to the InAs/InP material system with successful device demonstrations and high performance. In recent years, QD research has expanded into shorter wavelength material combinations,[119] the antimonides,[120] and tensile strained regimes,[121] which may one day yield promising devices at additional wavelengths. InAs dots on Si are also poised to finally achieve the decades-long goal of epitaxial III–V light sources on silicon, but more work remains to be done to prove high temperature reliability and, ideally, to enable photonic integration with other silicon photonic devices.

Quantum dot lasers are poised to make significant advancements in the next few years, particularly in the areas of photonic integrated circuits and in achieving high reliability for epitaxial integration on silicon. Their insensitivity to optical feedback is unprecedented and will enable functionalities and performance previously unachievable due to the lack of cheap, low loss, and/or integrated on-chip optical isolators. Current results also suggest that a clear path exists to close the gap between the native substrate and epitaxially grown on Si laser performance, which will open new doors to scalable, low cost manufacturing, thus increasing the application space that can be addressed with integrated photonics. Given the groundwork already laid in the development of integrated QW lasers, advancements in QD lasers are expected to be rapid.

DATA AVAILABILITY

The data that support the findings of this study are available from the corresponding author upon reasonable request.

REFERENCES

[1]Y. Arakawa and H. Sakaki, Appl. Phys. Lett. **40**, 939 (1982).
[2]M. Asada, Y. Miyamoto, and Y. Suematsu, IEEE J. Quantum Electron. **22**, 1915 (1986).
[3]M. Krishnamurthy, J. Drucker, and J. Venables, J. Appl. Phys. **69**, 6461 (1991).
[4]D. Leonard, private communication (2020).
[5]D. Leonard, M. Krishnamurthy, S. Fafard, J. Merz, and P. Petroff, J. Vac. Sci. Technol. B **12**, 1063 (1994).
[6]D. Leonard, M. Krishnamurthy, C. Reaves, S. P. DenBaars, and P. M. Petroff, Appl. Phys. Lett. **63**, 3203 (1993).
[7]J. Moison, F. Houzay, F. Barthe, L. Leprince, E. Andre, and O. Vatel, Appl. Phys. Lett. **64**, 196 (1994).
[8]L. Goldstein, F. Glas, J. Marzin, M. Charasse, and G. Le Roux, Appl. Phys. Lett. **47**, 1099 (1985).
[9]W. Schaffer, M. Lind, S. Kowalczyk, and R. Grant, J. Vac. Sci. Technol. B **1**, 688 (1983).
[10]J.-Y. Marzin, J.-M. Gérard, A. Izraël, D. Barrier, and G. Bastard, Phys. Rev. Lett. **73**, 716 (1994).

[11]M. Grundmann *et al.*, Phys. Rev. Lett. **74**, 4043 (1995).

[12]R. Mirin, J. Ibbetson, K. Nishi, A. Gossard, and J. Bowers, Appl. Phys. Lett. **67**, 3795 (1995).

[13]K. Kamath, P. Bhattacharya, T. Sosnowski, T. Norris, and J. Phillips, Electron. Lett. **32**, 1374 (1996).

[14]R. Mirin, A. Gossard, and J. Bowers, Electron. Lett. **32**, 1732 (1996).

[15]H. Shoji, Y. Nakata, K. Mukai, Y. Sugiyama, M. Sugawara, N. Yokoyama, and H. Ishikawa, Electron. Lett. **32**, 2023 (1996).

[16]N. Kirstaedter *et al.*, Appl. Phys. Lett. **69**, 1226 (1996).

[17]D. Huffaker, G. Park, Z. Zou, O. Shchekin, and D. Deppe, Appl. Phys. Lett. **73**, 2564 (1998).

[18]Z. I. Alferov, Sov. Phys. Semicond. **3**, 1107 (1970).

[19]Z. I. Alferov, V. Andreev, D. Garbuzov, Y. V. Zhilyaev, E. Morozov, E. Portnoi, and V. Trofim, Sov. Phys. Semicond. **4**, 1573 (1971).

[20]R. Miller, R. Dingle, A. Gossard, R. Logan, W. Nordland, Jr., and W. Wiegmann, J. Appl. Phys. **47**, 4509 (1976).

[21]R. D. Dupuis, P. Dapkus, N. Holonyak, Jr., E. Rezek, and R. Chin, Appl. Phys. Lett. **32**, 295 (1978).

[22]W. Tsang, Appl. Phys. Lett. **39**, 786 (1981).

[23]W. Tsang, Appl. Phys. Lett. **40**, 217 (1982).

[24]Z. I. Alferov, A. Vasiliev, S. Ivanov, P. Kop'ev, N. Ledentsov, B. Y. Meltser, and V. Ustinov, Sov. Phys. Techn. Phys. Lett. **14**, 782 (1988).

[25]N. Chand, E. Becker, J. Van der Ziel, S. G. Chu, and N. Dutta, Appl. Phys. Lett. **58**, 1704 (1991).

[26]N. Ledentsov *et al.*, Phys. Rev. B **54**, 8743 (1996).

[27]G. Liu, A. Stintz, H. Li, K. Malloy, and L. Lester, Electron. Lett. **35**, 1163 (1999).

[28]I. Sellers, H. Liu, K. Groom, D. Childs, D. Robbins, T. Badcock, M. Hopkinson, D. Mowbray, and M. Skolnick, Electron. Lett. **40**, 1412 (2004).

[29]J. Kim, T. Strand, R. Naone, and L. Coldren, Appl. Phys. Lett. **74**, 2752 (1999).

[30]A. Y. Liu, J. Peters, X. Huang, D. Jung, J. Norman, M. L. Lee, A. C. Gossard, and J. E. Bowers, Opt. Lett. **42**, 338 (2017).

[31]J. C. Norman, D. Jung, Y. Wan, and J. E. Bowers, APL Photonics **3**, 030901 (2018).

[32]Z. I. Alferov, Rev. Mod. Phys. **73**, 767 (2001).

[33]D. Bimberg and U. W. Pohl, Mater. Today **14**, 388 (2011).

[34]V. Shchukin, N. N. Ledentsov, and D. Bimberg, *Epitaxy of Nanostructures* (Springer Science & Business Media, Berlin, Heidelberg, 2013).

[35]G. Eisenstein and D. Bimberg, *Green Photonics and Electronics* (Springer, Berlin, Heidelberg, 2017).

[36]D. Bimberg, M. Grundmann, and N. N. Ledentsov, *Quantum Dot Heterostructures* (John Wiley & Sons, Chichester, West Sussex, 1999).

[37]M. Grundmann, *Nano-optoelectronics: Concepts, Physics and Devices* (Springer Science & Business Media, Berlin, Heidelberg, 2002).

[38]J. Wu, S. Chen, A. Seeds, and H. Liu, J. Phys. D: Appl. Phys. **48**, 363001 (2015).

[39]S. Pan, V. Cao, M. Liao, Y. Lu, Z. Liu, M. Tang, S. Chen, A. Seeds, and H. Liu, J. Semicond. **40**, 101302 (2019).

[40]J. C. Norman *et al.*, IEEE J. Quantum Electron. **55**, 1 (2019).

[41]P. Bhattacharya, S. Ghosh, and A. Stiff-Roberts, Annu. Rev. Mater. Res. **34**, 1 (2004).

[42]Z. Mi, J. Yang, P. Bhattacharya, G. Qin, and Z. Ma, Proc. IEEE **97**, 1239 (2009).

[43]O. Stier, M. Grundmann, and D. Bimberg, Phys. Rev. B **59**, 5688 (1999).

[44]O. Shchekin, J. Ahn, and D. Deppe, Electron. Lett. **38**, 712 (2002).

[45]O. Shchekin and D. Deppe, Appl. Phys. Lett. **80**, 3277 (2002).

[46]T. Kageyama *et al.*, *The European Conference on Lasers and Electro-Optics (CLEO)*, Munich, 22–26 May 2011 (Optical Society of America, Washington, DC, 2011).

[47]A. Abdollahinia *et al.*, Opt. Express **26**, 6056 (2018).

[48]Y. Urino, N. Hatori, K. Mizutani, T. Usuki, J. Fujikata, K. Yamada, T. Horikawa, T. Nakamura, and Y. Arakawa, J. Lightwave Technol. **33**, 1223 (2015).

[49]N. Ledentsov, L. Chorchos, O. Makarov, J.-R. Kropp, V. Shchukin, V. Kalosha, J. Turkiewicz, N. Cherkashin, and N. Ledentsov, Proc. SPIE **11300**, 113000H (2015).

[50]A. Y. Liu, C. Zhang, J. Norman, A. Snyder, D. Lubyshev, J. M. Fastenau, A. W. Liu, A. C. Gossard, and J. E. Bowers, Appl. Phys. Lett. **104**, 041104 (2014).

[51]C. Gilfert, V. Ivanov, N. Oehl, M. Yacob, and J. Reithmaier, Appl. Phys. Lett. **98**, 201102 (2011).

[52]M. Osinski and J. Buus, IEEE J. Quantum Electron. **23**, 9 (1987).

[53]L. A. Coldren, S. W. Corzine, and M. L. Mashanovitch, *Diode Lasers and Photonic Integrated Circuits* (John Wiley & Sons, Hoboken, New Jersey, 2012).

[54]M. Willatzen, T. Tanaka, Y. Arakawa, and J. Singh, IEEE J. Quantum Electron. **30**, 640 (1994).

[55]W. W. Chow and F. Jahnke, Prog. Quantum Electron. **37**, 109 (2013).

[56]T. Newell, D. Bossert, A. Stintz, B. Fuchs, K. Malloy, and L. Lester, IEEE Photon. Technol. Lett. **11**, 1527 (1999).

[57]W. W. Chow, Z. Zhang, J. C. Norman, S. Liu, and J. E. Bowers, APL Photonics **5**, 026101 (2020).

[58]J. Duan, H. Huang, Z. Lu, P. Poole, C. Wang, and F. Grillot, Appl. Phys. Lett. **112**, 121102 (2018).

[59]T. Septon *et al.*, Optica **6**, 1071 (2019).

[60]Y. Wan *et al.*, Laser Photonics Rev. **14**, 2000037 (2020).

[61]D. G. Deppe, H. Huang, and O. B. Shchekin, IEEE J. Quantum Electron. **38**, 1587 (2002).

[62]F. Lelarge *et al.*, IEEE J. Sel. Top. Quantum Electron. **13**, 111 (2007).

[63]A. Capua, L. Rozenfeld, V. Mikhelashvili, G. Eisenstein, M. Kuntz, M. Laemmlin, and D. Bimberg, Opt. Express **15**, 5388 (2007).

[64]J. Duan *et al.*, Opt. Lett. **45**, 4887 (2020).

[65]J. Helms and K. Petermann, IEEE J. Quantum Electron. **26**, 833 (1990).

[66]J. Duan, H. Huang, B. Dong, D. Jung, J. C. Norman, J. E. Bowers, and F. Grillot, IEEE Photon. Technol. Lett. **31**, 345 (2019).

[67]J. Duan, H. Huang, D. Jung, Z. Zhang, J. Norman, J. Bowers, and F. Grillot, Appl. Phys. Lett. **112**, 251111 (2018).

[68]F. Grillot, J. C. Norman, J. Duan, Z. Zhang, B. Dong, H. Huang, W. W. Chow, and J. E. Bowers, Nanophotonics **1**, 1271–1286 (2020).

[69]Z. Zhang, D. Jung, J. Norman, W. W. Chow, and J. E. Bowers, IEEE J. Sel. Top. Quantum Electron. **25**, 1–9 (2019).

[70]J. Duan, H. Huang, B. Dong, J. C. Norman, Z. Zhang, J. E. Bowers, and F. Grillot, Photonics Res. **7**, 1222 (2019).

[71]W. W. Chow, S. Liu, Z. Zhang, J. E. Bowers, and M. Sargent, Opt. Express **28**, 5317 (2020).

[72]D. Arsenijević and D. Bimberg, in *Green Photonics and Electronics*, edited by G. Eisenstein and D. Bimberg (Springer, Berlin, Heidelberg, 2017), p. 75.

[73]Z. Lu, J. Liu, P. Poole, Z. Jiao, P. Barrios, D. Poitras, J. Caballero, and X. Zhang, Opt. Commun. **284**, 2323 (2011).

[74]S. Liu, D. Jung, J. Norman, M. Kennedy, A. Gossard, and J. Bowers, Electron. Lett. **54**, 432 (2018).

[75]Z. Lu, J. Liu, S. Raymond, P. Poole, P. Barrios, and D. Poitras, Opt. Express **16**, 10835 (2008).

[76]F. Gao, S. Luo, H.-M. Ji, S.-T. Liu, F. Xu, Z.-R. Lv, D. Lu, C. Ji, and T. Yang, IEEE Photonics Technol. Lett. **28**, 1481 (2016).

[77]J. Renaudier *et al.*, Electron. Lett. **41**, 1007 (2005).

[78]D. Jung, J. Norman, Y. Wan, S. Liu, R. Herrick, J. Selvidge, K. Mukherjee, A. C. Gossard, and J. E. Bowers, Phys. Status Solidi A **216**, 1800602 (2019).

[79]G. Liu, Z. Lu, J. Liu, Y. Mao, M. Vachon, C. Song, and P. J. Poole, *Presented at the Optical Fiber Communication Conference*, San Diego, California, 11 March 2020 (Optical Society of America, 2020).

[80]Z. Lu, J. Liu, L. Mao, C.-Y. Song, J. Weber, D. Poitras, and P. Poole, Proc. SPIE **10946**, 109460A (2019).

[81]X. Huang, A. Stintz, H. Li, L. Lester, J. Cheng, and K. Malloy, Appl. Phys. Lett. **78**, 2825 (2001).

[82]G. Carpintero, M. G. Thompson, R. V. Penty, and I. H. White, IEEE Photon. Technol. Lett. **21**, 389 (2009).

[83]L. Drzewietzki, S. Breuer, and W. Elsäßer, Opt. Express **21**, 16142 (2013).

[84]F. Kéfélian, S. O'Donoghue, M. T. Todaro, J. G. McInerney, and G. Huyet, IEEE Photon. Technol. Lett. **20**, 1405 (2008).

[85]C.-Y. Lin, F. Grillot, Y. Li, R. Raghunathan, and L. F. Lester, Opt. Express **18**, 21932 (2010).

[86]S. Liu, X. Wu, D. Jung, J. C. Norman, M. Kennedy, H. K. Tsang, A. C. Gossard, and J. E. Bowers, Optica **6**, 128 (2019).

[87]S. Meinecke, L. Drzewietzki, C. Weber, B. Lingnau, S. Breuer, and K. Lüdge, Sci. Rep. **9**, 1783 (2019).

[88]E. Rafailov, M. Cataluna, and W. Sibbett, Nat. Photonics **1**, 395 (2007).

[89]R. Rosales, K. Merghem, A. Martinez, A. Akrout, J.-P. Tourrenc, A. Accard, F. Lelarge, and A. Ramdane, IEEE J. Sel. Top. Quantum Electron. **17**, 1292 (2011).

[90]H. Schmeckebier, G. Fiol, C. Meuer, D. Arsenijević, and D. Bimberg, Opt. Express **18**, 3415 (2010).

[91]M. G. Thompson, A. R. Rae, M. Xia, R. V. Penty, and I. H. White, IEEE J. Sel. Top. Quantum Electron. **15**, 661 (2009).

[92]C. Weber et al., Opt. Lett. **40**, 395 (2015).

[93]R. Rosales, K. Merghem, C. Calo, G. Bouwmans, I. Krestnikov, A. Martinez, and A. Ramdane, Appl. Phys. Lett. **101**, 221113 (2012).

[94]Z. Lu, J. Liu, P. Poole, C. Song, and S. Chang, Opt. Express **26**, 11909 (2018).

[95]S. Liu, J. C. Norman, D. Jung, M. Kennedy, A. C. Gossard, and J. E. Bowers, Appl. Phys. Lett. **113**, 041108 (2018).

[96]D. Auth, S. Liu, J. Norman, J. E. Bowers, and S. Breuer, Opt. Express **27**, 27256 (2019).

[97]K. Merghem, A. Akrout, A. Martinez, G. Aubin, A. Ramdane, F. Lelarge, and G.-H. Duan, Appl. Phys. Lett. **94**, 021107 (2009).

[98]M. Zeiler, IEEE Potentials **35**, 36 (2016).

[99]O. Ueda and S. J. Pearton, *Materials and Reliability Handbook for Semiconductor Optical and Electron Devices* (Springer Science & Business Media, New York, 2012).

[100]J. Selvidge, J. Norman, M. E. Salmon, E. T. Hughes, J. E. Bowers, R. Herrick, and K. Mukherjee, Appl. Phys. Lett. **115**, 131102 (2019).

[101]A. Y. Liu, S. Srinivasan, J. Norman, A. C. Gossard, and J. E. Bowers, Photonics Res. **3**, B1 (2015).

[102]Z. Liu et al., J. Lightwave Technol. **38**, 240–248 (2020).

[103]C. Hantschmann, M. Tang, S. Chen, A. J. Seeds, H. Liu, I. White, and R. Penty, J. Lightwave Technol. **38**, 4801–4807 (2020).

[104]R. W. Herrick, D. Jung, A. Liu, J. Norman, C. Jan, and J. Bowers, *2017 IEEE Photonics Conference (IPC)*, Orlando, FL, 1–5 October 2017 (IEEE, New York, 2017).

[105]R. Herrick and O. Ueda, *Reliability of Semiconductor Lasers and Optoelectronic Devices*, 1st ed. (Woodhead Publishing, Sawston, Cambridge, 2021).

[106]D. Jung, R. Herrick, J. Norman, K. Turnlund, C. Jan, K. Feng, A. C. Gossard, and J. E. Bowers, Appl. Phys. Lett. **112**, 153507 (2018).

[107]S. Chen et al., Nat. Photonics **10**, 307 (2016).

[108]J. C. Norman, Z. Zhang, D. Jung, C. Shang, M. Kennedy, M. Dumont, R. W. Herrick, A. C. Gossard, and J. E. Bowers, IEEE J. Quantum Electron. **55**, 1 (2019).

[109]K. Mukherjee, J. Selvidge, D. Jung, J. Norman, A. A. Taylor, M. Salmon, A. Y. Liu, J. E. Bowers, and R. W. Herrick, J. Appl. Phys. **128**, 025703 (2020).

[110]M. Buffolo et al., IEEE J. Quantum Electron. **55**, 1 (2019).

[111]M. Buffolo et al., IEEE J. Sel. Top. Quantum Electron. **26**, 1 (2019).

[112]D. Jung, J. Norman, Y. Wan, S. Liu, R. Herrick, J. Selvidge, K. Mukherjee, A. C. Gossard, and J. E. Bowers, Phys. Status Solidi A **216**, 1800602 (2018).

[113]A. Y. Liu, R. W. Herrick, O. Ueda, P. M. Petroff, A. C. Gossard, and J. E. Bowers, IEEE J. Sel. Top. Quantum Electron. **21**, 690 (2015).

[114]J. Selvidge et al., Appl. Phys. Lett. **117**, 122101 (2020).

[115]J. Norman, Z. Zhang, D. Jung, C. Shang, M. Kennedy, M. Dumont, R. Herrick, A. Gossard, and J. Bowers, IEEE J. Quantum Electron. **55**, 2001111 (2019).

[116]J. C. Norman et al., Proc. SPIE **11285**, 1128504 (2020).

[117]N. Sobolev, A. Cavaco, M. Carmo, M. Grundmann, F. Heinrichsdorff, and D. Bimberg, Phys. Status Solidi B **224**, 93 (2001).

[118]P. Piva, R. Goldberg, I. Mitchell, D. Labrie, R. Leon, S. Charbonneau, Z. Wasilewski, and S. Fafard, Appl. Phys. Lett. **77**, 624 (2000).

[119]K. Rivoire, S. Buckley, Y. Song, M. L. Lee, and J. Vučković, Phys. Rev. B **85**, 045319 (2012).

[120]Q. Lu, Q. Zhuang, J. Hayton, M. Yin, and A. Krier, Appl. Phys. Lett. **105**, 031115 (2014).

[121]P. J. Simmonds, C. D. Yerino, M. Sun, B. Liang, D. L. Huffaker, V. G. Dorogan, Y. Mazur, G. Salamo, and M. L. Lee, ACS Nano **7**, 5017 (2013).